

Light nuclei v_1 and v_2 in Au+Au collisions at $\sqrt{s_{NN}} = 3$ GeV from STAR

Xionghong He (for the STAR collaboration)*

Institute of Modern Physics, Chinese Academy of Sciences

E-mail: hexh@impcas.ac.cn

Comprehensive measurements of light nuclei collectivity provide valuable information for understanding light nuclei production mechanism in heavy-ion collisions. The v_1 and v_2 for deuterons, tritons, ^3He , and ^4He have been measured in Au+Au collisions at $\sqrt{s_{NN}} = 3$ GeV by the STAR experiment at RHIC. The data was recorded in fixed-target mode in 2018. The particle rapidity and transverse momentum dependence of v_1 and v_2 for these particles have been shown. These results are qualitatively consistent with the calculations from the JAM transport model plus nucleon coalescence.

The International conference on Critical Point and Onset of Deconfinement (CPOD2021)

March 15 - March 19, 2021

Online Meeting

*Speaker.

1. Introduction

Study of light nuclei production in heavy-ion collisions, to understand their production mechanism and the underlying collision dynamics, is of particular interest for both theoretical and experimental efforts [1]. The production mechanism of light nuclei in relativistic heavy-ion collisions is still under debate. There are several popular theoretical models: thermal model, coalescence model, and dynamical model, see the review [2]. The coalescence model assumes that the light nuclei are formed via the combination of nucleons, when these nucleons are near each other both in coordinate and momentum spaces [3, 4, 5]. One general feature of the nucleon coalescence model is that the light nucleus collective flow is expected to follow an atomic-mass-number A scaling [6]

$$v_n^A(p_T) \approx v_n^p(p_T/A),$$

where n represents the n -th order collective flow and v_n^p is proton collective flow. Thus, comprehensive measurements of light nuclei directed flow, v_1 , and elliptic flow, v_2 , provide valuable information on the nucleon coalescence sum rule and will help better understand light nuclei production mechanism in such collisions. Light nuclei v_2 measured by STAR [7] follows the A scaling at $p_T/A < 1.5$ GeV/ c from $\sqrt{s_{NN}} = 7.7 - 200$ GeV Au+Au collisions, which is consistent with the picture of nucleon coalescence production mechanism for light nuclei. In the collision energy regime of a few GeV, the relatively long passing time of the two colliding nuclei naturally leads to interactions between the spectator matter and the fireball. Therefore, the light nuclei flow pattern may be strongly affected by the spectator fragments.

2. Analysis

The data used in this measurement were collected in the fixed-target Au+Au collisions program by the STAR experiment [8]. The beam energy is 3.85 GeV per nucleon, which gives a center-of-mass energy of $\sqrt{s_{NN}} = 3.0$ GeV. For the fixed target configuration of STAR experiment, the Au target is installed inside the vacuum pipe and 2.0 m to the west of center of Time Projection Chamber (TPC) [9]. The light nuclei identification is accomplished by the energy loss dE/dx measured in the TPC. A combination of TPC and Time of Flight [10] detectors is used to identify the high momentum p , d , t , and ${}^4\text{He}$.

The flow coefficients v_1 and v_2 are determined via the particle momentum azimuthal angle relative to the azimuth of the first-order event-plane Ψ_1 [11]. The Ψ_1 is reconstructed by using the hit information in the event-plane detector (EPD). A standard shifting method [11] is utilized to make the distribution of the reconstructed Ψ_1 isotropic. The Ψ_1 resolution is determined by three sub-event-plane correlation method [11], where the sub-event planes are reconstructed separately in different η ranges of EPD and TPC. The final v_1 and v_2 values are obtained after correcting for the efficiency and event-plane resolution.

3. Results

3.1 p_T dependence of light nuclei v_1 and v_2

Figure 1 (a) is the p_T dependence of light nuclei v_1 in four rapidity intervals in 10-40% Au+Au

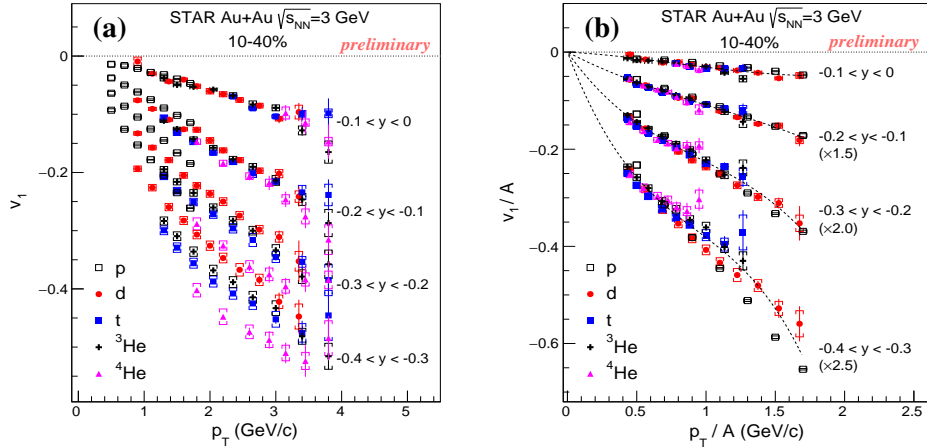


Figure 1: The v_1 as a function of p_T for p , d , t , ${}^3\text{He}$, and ${}^4\text{He}$ in four rapidity intervals in 10-40% Au+Au collisions without (a) and with (b) A scaled, respectively. Statistical and systematic uncertainties are represented by vertical lines and open boxes separately. The dashed lines are used to guide the eyes.

37 collisions. In the plot (b), the value v_1 and p_T are scaled by A to validate the coalescence model. It
 38 is observed that the v_1/A of all the light nuclei follow the A scaling within $-0.3 < y < 0$. The v_1
 39 scaling behavior suggests that the light nuclei are formed via the nucleon coalescence in Au+Au
 40 collisions at $\sqrt{s_{NN}} = 3$ GeV. In $-0.4 < y < -0.3$, the scaling is violated at $p_T/A > 1$ GeV/ c , which
 41 may be caused by the fragments close to the target rapidity.

42 Figure 2 is the p_T dependence of v_2 for light nuclei in four rapidity intervals. At mid-rapidity
 43 $-0.1 < y < 0$, the v_2 values are negative for all the measured light nuclei species. Moving away
 44 from mid-rapidity, the v_2 of p and d stay negative within $-0.4 < y < 0$, while the v_2 for t , ${}^3\text{He}$, and
 45 ${}^4\text{He}$ increase gradually and become positive at larger transverse momenta. At $-0.4 < y < -0.2$,
 46 the v_2 of p and d have different sign from those of t , ${}^3\text{He}$, and ${}^4\text{He}$. Moreover, the proton v_2 has
 47 a stronger non-monotonic p_T dependence compared to other light nuclei. The light nucleus v_2
 48 violate the A scaling at $\sqrt{s_{NN}} = 3$ GeV, which is different from the A scaling observed for $p_T/A <$
 49 1.5 GeV/ c in higher energy $\sqrt{s_{NN}} = 7.7 - 200$ GeV Au+Au collisions [7].

50 3.2 Rapidity dependence of light nuclei v_1 and v_2

51 Figure 3 shows p_T integrated v_1 and v_2 distributions as a function of particle rapidity in 10-
 52 40% Au+Au collisions at $\sqrt{s_{NN}} = 3$ GeV. The proton results are obtained in $0.4 < p_T < 2.0$ GeV/ c .
 53 The low limits of light nuclei p_T are determined to be the same p_T/A as protons. The upper limits
 54 of p_T are determined by the acceptance of each light nuclei species within $-0.5 < y < 0$. There
 55 are clear mass ordering for both v_1 and v_2 . The heavier nuclei have stronger rapidity dependence
 56 in v_1 . At mid-rapidity $-0.1 < y < 0$, the value of v_2 is negative and nearly identical for all light
 57 nuclei species. The negative v_2 at mid-rapidity may be caused by a shadowing of the spectators as
 58 their passage time is comparable with the expansion time of collision system at $\sqrt{s_{NN}} = 3$ GeV.
 59 Away from the mid-rapidity, the proton v_2 remains negative and those of other light nuclei become
 60 positive, which means no more A scaling.

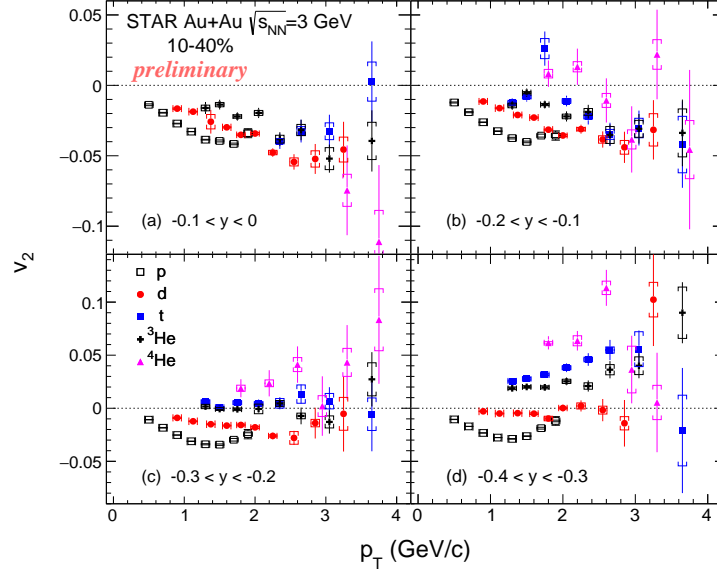


Figure 2: The v_2 as a function of p_T for p , d , t , ${}^3\text{He}$, and ${}^4\text{He}$ in four rapidity intervals in 10-40% Au+Au collisions. Statistical and systematic uncertainties are represented by vertical lines and open boxes separately.

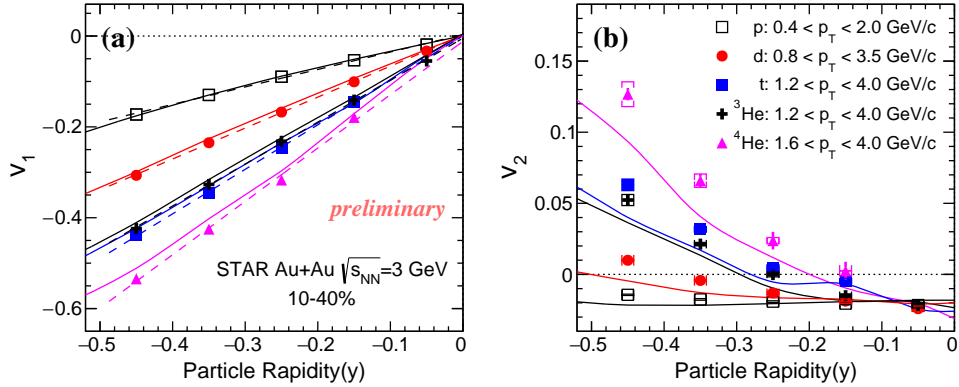


Figure 3: The v_1 (a) and v_2 (b) as a function of rapidity for p , d , t , ${}^3\text{He}$, and ${}^4\text{He}$ in selected p_T ranges in 10-40% Au+Au collisions. The dashed lines are the fit to v_1 with first-order polynomial functions. The solid lines are the calculations from JAM transport model plus nucleon coalescence.

61 A transport model, Jet AA Microscopic Transportation Model (JAM) [12], is utilized to sim-
 62 ulate Au+Au collisions from initial collision stage to final hadron transport at $\sqrt{s_{NN}} = 3$ GeV. A
 63 baryonic mean-field with momentum dependent potential is used in the simulation. Then the light
 64 nuclei are formed by the coalescence of the proton and neutron according to their phase-space
 65 distributions from above simulation. The coalescence condition is that the relative momenta to be
 66 $\Delta p < 0.3$ GeV/c and relative space distance to be $\Delta r < 4$ fm in their rest frame. The resulting
 67 v_1 and v_2 from the simulation are consistent with the experimental observations qualitatively, as
 68 shown by the solid-lines in Fig. 3. The sign change in v_2 of proton to light nuclei at larger rapidity

69 is also seen by the simulation.

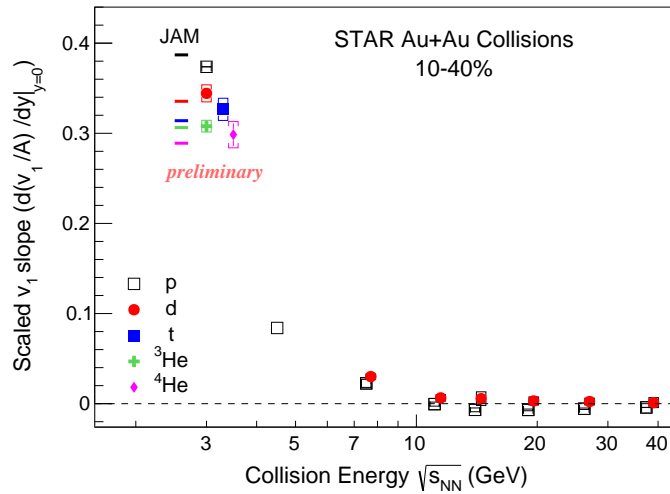


Figure 4: The light nuclei v_1 slope, dv_1/dy , as a function of collision energy $\sqrt{s_{NN}}$ in Au+Au collisions from STAR. The data points above 7 GeV are taken from [13]. The proton result at $\sqrt{s_{NN}} = 4.5$ GeV is for 10-25% Au+Au collisions [14].

70 A first-order polynomial function is employed to fit the v_1 distribution within rapidity range
 71 $-0.5 < y < 0$. The extracted slope parameters, dv_1/dy , scaled with A , for light nuclei are shown in
 72 Fig. 4. The values of $(dv_1/dy)/A$ for all measured light nuclei are close to each other at $\sqrt{s_{NN}} =$
 73 3 GeV considering the statistical and systematic uncertainties. The results of JAM model in mean-
 74 field mode plus coalescence calculations for p , d , t , ${}^3\text{He}$ and ${}^4\text{He}$ are consistent with the data. For
 75 energy $\sqrt{s_{NN}} > 7.7$ GeV, the value of proton dv_1/dy is negative and the corresponding slopes of
 76 deuteron v_1 are positive with larger uncertainties [13]. The different scaling behavior of light nuclei
 77 dv_1/dy at lower energies (≤ 7.7 GeV) and higher energies (> 11.5 GeV) may indicate different
 78 collision dynamics or different production mechanisms of light nuclei.

79 4. Summary

80 We report the measurements of v_1 and v_2 for d , t , ${}^3\text{He}$, and ${}^4\text{He}$ in 10-40% Au+Au collisions
 81 at $\sqrt{s_{NN}} = 3$ GeV. The light nucleus v_1 follows the atomic-mass-number scaling at rapidity $-0.5 <$
 82 $y < 0$, which is consistent with the nucleon coalescence picture. The values of light nuclei v_2 do
 83 not have a simple A scaling effect. The JAM model, with the baryon mean-field, and nucleon
 84 coalescence can qualitatively reproduce both the v_1 and v_2 for all light nuclei. Comparing with the
 85 high energy results, baryonic interactions may dominate the collision dynamics at 3 GeV Au+Au
 86 collisions.

87 References

- 88 [1] Peter Braun-Munzinger and Benjamin Dönigus, Nuclear Physics A, **987**, 144 (2019).
 89 [2] Dmytro Oliinychenko, Nuclear Physics A, **1005**, 121754 (2021).

- 90 [3] S. T. Butler and C. A. Pearson, Phys. Rev. **129**, 836 (1963).
- 91 [4] H. Sato and K. Yazaki, Phys. Lett. B **98**, 153 (1981).
- 92 [5] J. Steinheimer, K. Gudima, A. Botvina, I. Mishustin, M. Bleicher, and H. Stöcker, Phys. Lett. B **714**,
93 85 (2012).
- 94 [6] D. Molnár and S. A. Voloshin, Phys. Rev. Lett. **91**, 092301 (2003).
- 95 [7] L. Adamczyk *et al.* (STAR Collaboration), Phys. Rev. C **94**, 034908 (2016).
- 96 [8] K. H. Ackermann *et al.*, Nucl. Instrum. Meth. A **499**, 624 (2003).
- 97 [9] M. Anderson *et al.*, Nucl. Instrum. Meth. A **499**, 659 (2003).
- 98 [10] W. J. Llope, Nucl. Instrum. Meth. A **661**, S110, (2012).
- 99 [11] A. M. Poskanzer and S. A. Voloshin, Phys. Rev. C **58**, 1671 (1998).
- 100 [12] Y. Nara, N. Otuka, A. Ohnishi, K. Niita, S. Chiba, Phys. Rev. C **61**, 024901 (2000).
- 101 [13] J. Adam *et al.* (STAR Collaboration), Phys. Rev. C **102**, 044902 (2020).
- 102 [14] M. S. Abdallah *et al.* (STAR Collaboration), Phys. Rev. C **103**, 034908 (2021).